

Gravitational Wave Constraints on Planetary-Mass Primordial Black Holes Using LIGO O3a Data

Andrew L. Miller^{1,2,*}, Nancy Aggarwal^{3,†}, Sébastien Clesse⁴, Federico De Lillo⁵, Surabhi Sachdev⁶, Pia Astone⁷, Cristiano Palomba⁷, Ornella J. Piccinni⁸, and Lorenzo Pierini⁷

¹*Nikhef—National Institute for Subatomic Physics, Science Park 105, 1098 XG Amsterdam, The Netherlands*

²*Institute for Gravitational and Subatomic Physics (GRASP), Utrecht University, Princetonplein 1, 3584 CC Utrecht, The Netherlands*

³*University of California, Davis, Department of Physics, Davis, California 95616, USA*


⁴*Service de Physique Théorique, Université Libre de Bruxelles, Boulevard du Triomphe CP225, B-1050 Brussels, Belgium*

⁵*Université catholique de Louvain, B-1348 Louvain-la-Neuve, Belgium*

⁶*School of Physics, Georgia Institute of Technology, Atlanta, Georgia 30332, USA*

⁷*INFN, Sezione di Roma, I-00185 Roma, Italy*

⁸*OzGrav, Australian National University, Canberra, Australian Capital Territory 0200, Australia*

 (Received 1 March 2024; revised 14 May 2024; accepted 18 July 2024; published 10 September 2024)

Gravitational waves from subsolar mass inspiraling compact objects would provide almost smoking-gun evidence for primordial black holes (PBHs). We perform the first search for inspiraling planetary-mass compact objects in equal-mass and highly asymmetric mass-ratio binaries using data from the first half of the LIGO-Virgo-KAGRA third observing run. Though we do not find any significant candidates, we determine the maximum luminosity distance reachable with our search to be of $\mathcal{O}(0.1\text{--}100)$ kpc, and corresponding model-independent upper limits on the merger rate densities to be $\mathcal{O}(10^3\text{--}10^{-7})$ $\text{kpc}^{-3}\text{yr}^{-1}$ for systems with chirp masses of $\mathcal{O}(10^{-4}\text{--}10^{-2})M_{\odot}$, respectively. Furthermore, we interpret these rate densities as arising from PBH binaries and constrain the fraction of dark matter that such objects could comprise. For equal-mass PBH binaries, we find that these objects would compose less than 4%–100% of DM for PBH masses of $10^{-2}M_{\odot}$ to $2 \times 10^{-3}M_{\odot}$, respectively. For asymmetric binaries, assuming one black hole mass corresponds to a peak in the mass function at $2.5M_{\odot}$, a PBH dark-matter fraction of 10% and a second, much lighter PBH, we constrain the mass function of the second PBH to be less than 1 for masses between $1.5 \times 10^{-5}M_{\odot}$ and $2 \times 10^{-4}M_{\odot}$. Our constraints, recently released, are robust enough to be applied to *any* PBH or exotic compact object binary formation models, and complement existence microlensing results.

DOI: 10.1103/PhysRevLett.133.111401

Introduction—The detection of low-spinning black holes by LIGO, Virgo, and KAGRA [1–14] has renewed interest in primordial black holes (PBHs) as dark-matter (DM) candidates [15–17]. Depending on when and how PBHs formed in the early universe [18–23], they could have any mass between $\sim[10^{-18}, 10^9]M_{\odot}$, and could comprise a fraction f_{PBH} [17,24–26] or all of DM [15,16,18,20–22,27,28]. Such a wide mass range necessitates different probes of PBHs, one of which is through gravitational-wave (GW) emission. However, there is ambiguity between astrophysical and primordial formation mechanisms to explain observations of black holes above a solar mass [16,29]; hence, it is worthwhile to search for GWs from inspiraling compact objects below a solar mass, whose origins almost certainly would be primordial [30,31].

Despite a generic feature in the PBH mass function that appears at $10^{-5}M_{\odot}$ [18,19,32,33], much interest so far has

focused on subsolar mass (SSM) PBHs with masses between $[0.1, 1]M_{\odot}$ using matched filtering, the ideal, computationally intensive signal processing technique that correlates a huge number of waveforms with the data [34–40], with one exception [41]. While these searches have yielded no significant GW events (one search, however, claims to have seen a SSM low-significance candidate [42,43]), they have placed stringent upper limits on $f_{\text{PBH}} \lesssim \text{few}\%$.

However, GWs from PBH inspirals with masses $\lesssim 0.1M_{\odot}$ could spend at least hours in the detector frequency range, which is problematic for matched-filtering methods, since phase mismatch between templates accumulates with signal duration, thus requiring many more templates to cover the same parameter space [44]. Thus, we propose to search for such planetary-mass PBHs with a more computationally efficient method than matched filtering: the “generalized frequency Hough” [45–47].

Inspiraling planetary-mass PBH binaries could lead to detectable GW signals if they formed within our galaxy,

*Contact author: andrew.miller@nikhef.nl

†Contact author: nqagarwal@ucdavis.edu

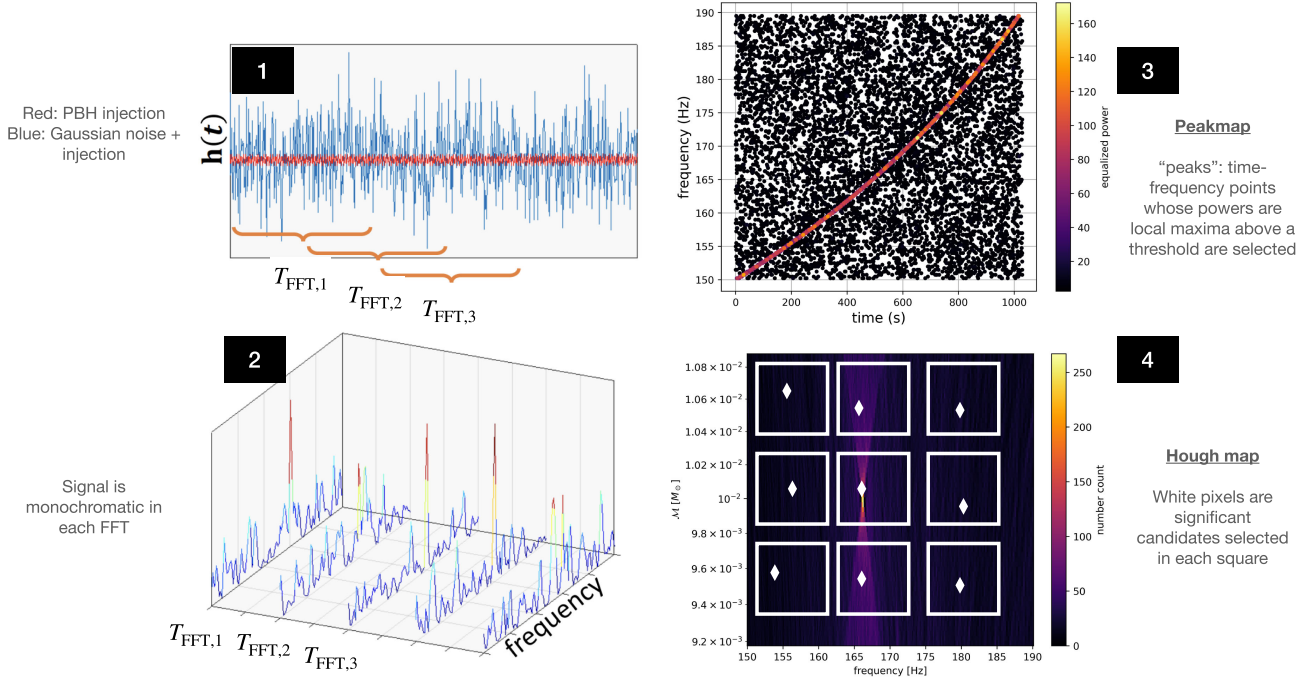


FIG. 1. Summary of our search for inspiraling PBH binaries. Step 1: perform 50% interlaced FFTs of length T_{FFT} , chosen such that the signal power is confined to one frequency bin in each FFT: $\dot{f}_{\text{gw}} T_{\text{FFT}} \leq (1/T_{\text{FFT}})$. Step 2: estimate the noise PSD and calculate the equalized power $|\text{FFT}|^2/\text{PSD}$. Step 3: select local maxima above a threshold $\theta_{\text{thr}} = 2.5$ to build the time-frequency peak map. Step 4: apply the generalized frequency Hough to find the most likely f_0 and \mathcal{M} of a PBH binary, and select significant candidates in different “squares” of the Hough map.

motivating the development of new methods to search for them [47–49]. Furthermore, recent detections of star and quasar microlensing events from HSC [50], OGLE [51], and EROS [52] have suggested that PBHs with masses between $10^{-6}M_{\odot}$ and $10^{-5}M_{\odot}$ could compose $\sim 2\%$ – 10% of DM [53,54]. However, microlensing limits could be evaded if PBHs form in clusters [18,26,55–58], thus we must probe the same PBH masses in different ways.

In this work, we perform the first-ever search for GWs from planetary-mass PBH binaries, and place the first GW constraints on the fraction of DM that planetary-mass PBHs could compose. Because our search is primarily sensitive to the chirp mass of the binary, we can constrain both equal-mass and asymmetric-mass ratio PBH binaries, the latter of which may form more often. Details of our search can be found in our companion paper [45].

Signal model—Inspiraling compact objects will emit GWs that shrink their orbits over time, leading to their eventual merger [59]. When two objects are far from merger, we can approximate the GW emission as arising from two point masses orbiting around their center of mass. Equating orbital energy loss with GW power, the rate of change of the GW frequency over time (the spin-up) \dot{f}_{gw} is [59]

$$\dot{f}_{\text{gw}} = \frac{96}{5} \pi^{8/3} \left(\frac{G\mathcal{M}}{c^3} \right)^{5/3} f_{\text{gw}}^{11/3} \equiv k f_{\text{gw}}^{11/3}. \quad (1)$$

$\mathcal{M} \equiv \{[(m_1 m_2)^{3/5}] / [(m_1 + m_2)^{1/5}]\}$ is the chirp mass of the system, f_{gw} is the GW frequency, c is the speed of light, and G is Newton’s gravitational constant. Integrating Eq. (1), we obtain the frequency evolution $f_{\text{gw}}(t)$:

$$f_{\text{gw}}(t) = f_0 \left[1 - \frac{8}{3} k f_0^{8/3} (t - t_0) \right]^{-3/8}, \quad (2)$$

where t_0 is a reference time for the GW frequency f_0 and t is the time at f_{gw} . The amplitude $h_0(t)$ from a source at a distance d away evolves as [59]

$$h_0(t) = \frac{4}{d} \left(\frac{G\mathcal{M}}{c^2} \right)^{5/3} \left(\frac{\pi f_{\text{gw}}(t)}{c} \right)^{2/3}. \quad (3)$$

While Eq. (1) represents the zeroth-order post-Newtonian (PN) term [59], because we observe the inspiral far from merger, our results are valid up to 3.5 PN for equal-mass and asymmetric-mass ratio systems with $q = m_2/m_1 \approx \eta \in [10^{-7}, 10^{-4}]$ in this parameter space [49] assuming $m_1 \sim \mathcal{O}(M_{\odot})$.

Search—Method: We begin with six months of cleaned, calibrated LIGO O3a strain data $h(t)$ [60–64] that we divide into chunks of length T_{FFT} , which we fast Fourier transform (FFT). In each FFT, we estimate the level of the background noise power spectral density (PSD), and

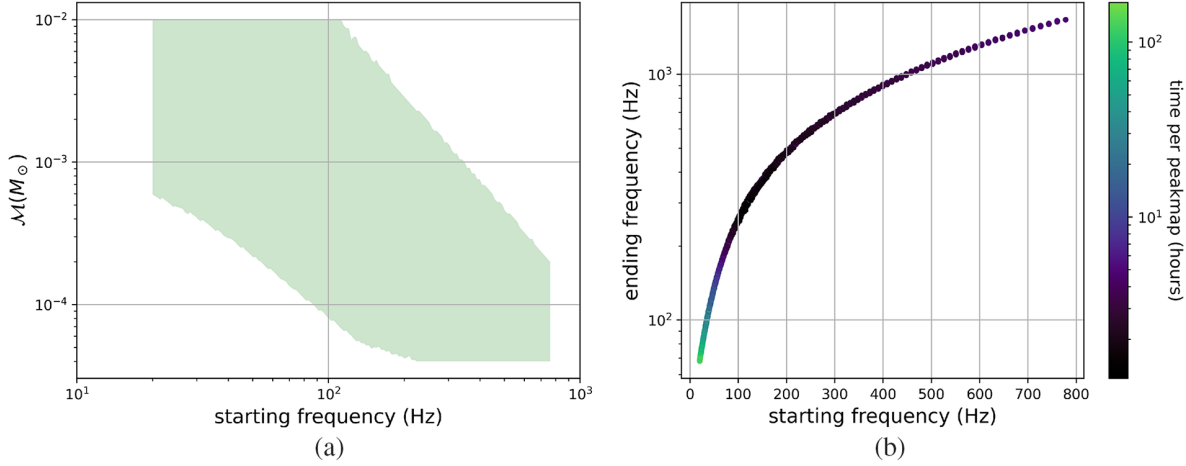


FIG. 2. Left: the chirp mass range probed in our search as a function of f_0 . The shape results because we analyze only systems that could be detected at least 0.1 kpc away at 95% confidence. Right: T_{PM} as a function of frequency range analyzed in this search. $T_{\text{FFT}} \in [2, 29]$ s.

divide the square modulus of the FFT by the PSD to obtain the “equalized power” [45], which has mean and standard deviation equal to one in Gaussian noise [65].

We repeat this procedure for each FFT to build a time-frequency peak map, in which any “peak” (a time-frequency point) whose power has exceeded a threshold $\theta_{\text{thr}} = 2.5$ is labeled with “1.” This peak map is the input to the generalized frequency Hough, which maps peaks in the time-frequency plane to lines in the frequency-chirp mass plane.

To apply the generalized frequency Hough, we must linearize the peak map by setting $z = f_{\text{gw}}^{-8/3}$ in Eq. (2), resulting in $z = z_0 - \frac{8}{3}k(t - t_0)$, where $z_0 = f_0^{-8/3}$ [46]. Our method sums the 1s in the $t-z$ plane along different linear tracks, not the power, to avoid being blinded by noise disturbances [65,66], and results in a two-dimensional histogram in the $z_0 - k$ ($f_0 - \mathcal{M}$) plane, called the “Hough map.” We show a schematic of the search in Fig. 1.

We plot in Fig. 2(a) the searched parameter space, which extends a few orders of magnitude lower in chirp mass than that in previous SSM searches [38–40]. In Fig. 2(b), we show T_{PM} , the duration of each peak map, as a function of starting and ending frequency of each analyzed band. We choose the frequency band, T_{FFT} and T_{PM} to maximize sensitivity to particular chirp-mass systems [45], and thus run the search in $N_{\text{config}} = 129$ configurations. Each configuration corresponds to creating $N_{\text{PM}} = T_{\text{obs}}/T_{\text{PM}}$ peak maps and running the generalized frequency Hough on each one.

Candidates and follow-up: We analyze data from LLO and LHO separately, and select strong “candidates,” particular z_0 and k values, whose number counts in the Hough map are high with respect to those in nearby $z_0 - k$ pixels, and find $\sim 10^7$ coincident candidates. A “coincidence” occurs if the Pythagorean distance between the returned

z_0 and k of candidates from each detector are within 3 bins [46] at the same t_0 [45]. For each candidate, we calculate the critical ratio CR , our detection statistic: $CR = [(m - \mu)/\sigma]$, where m is the number count of each candidate in the Hough map, and μ and σ are the mean and standard deviation, respectively, of the number counts in different squares of the Hough map [45].

We define a configuration-dependent threshold CR [45] above which we decide candidates are “significant.” We determine if the remaining 7457 candidates are real by returning to $h(t)$ and correcting the data for the phase evolution of these candidates, a process called “heterodyning” [45,67]. If the candidate parameters match the signal parameters in the data, heterodyning results in a monochromatic signal, allowing us to take a longer T_{FFT} , which leads to a larger CR . No candidate survived heterodyning.

Upper limits—Constraints on rate density: We compute upper limits using a hybrid theoretical or data-driven approach that has been verified through injections [45]. The sensitivity of the generalized frequency Hough search towards inspiraling binary systems has been computed in [47] in terms of the maximum distance reach d_{max} at confidence level $\Gamma = 0.95$:

$$d_{\text{max}} = \left(\frac{GM}{c^2}\right)^{5/3} \left(\frac{\pi}{c}\right)^{2/3} \frac{T_{\text{FFT}}}{\sqrt{T_{\text{PM}}}} \left(\sum_x^N \frac{f_{\text{gw},x}^{4/3}}{S_n(f_{\text{gw},x})}\right)^{1/2} \times \left(\frac{p_0(1-p_0)}{Np_1^2}\right)^{-1/4} \sqrt{\frac{\theta_{\text{thr}}}{(CR - \sqrt{2}\text{erfc}^{-1}(2\Gamma))}}. \quad (4)$$

Here, $p_0 = e^{-\theta_{\text{thr}}} - e^{-2\theta_{\text{thr}}} + \frac{1}{3}e^{-3\theta_{\text{thr}}}$ is the probability of selecting a peak above θ_{thr} , $p_1 = e^{-\theta_{\text{thr}}} - 2e^{-2\theta_{\text{thr}}} + e^{-3\theta_{\text{thr}}}$, $N = T_{\text{PM}}/T_{\text{FFT}}$, and S_n is the averaged LHO/LLO noise PSD in O3a, given in [45]. x indicates the sum over the

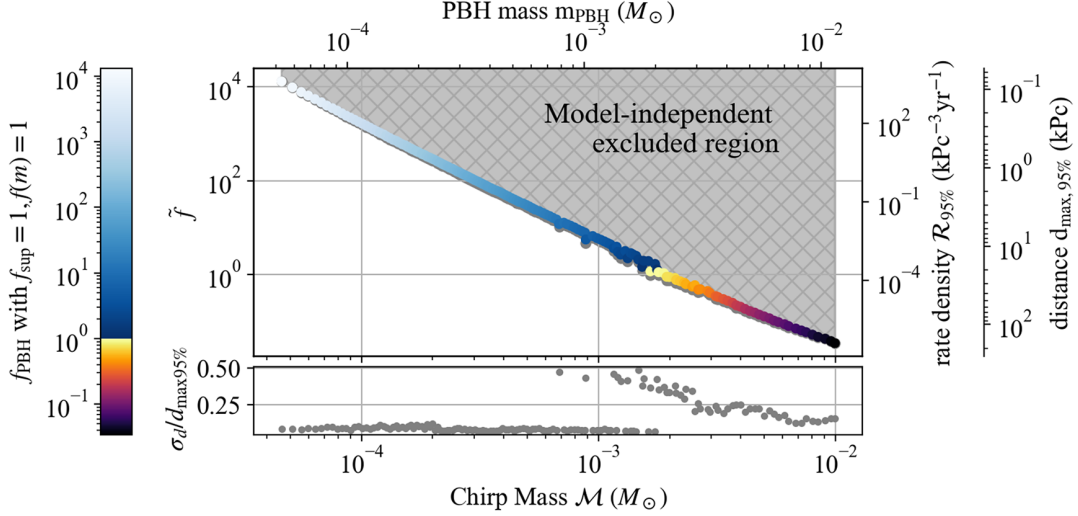


FIG. 3. For equal-mass binaries, upper limits on \tilde{f} (left y axis), the merger rate density (right y axis), and maximum distance reach (rightmost y axis) as a function of chirp mass (lower x axis) and PBH mass (upper x axis). Gray-hatched regions denote model-independent constraints on \tilde{f} , distances and rate densities that are excluded by this analysis of O3a LIGO data. Model-dependent limits on f_{PBH} are shown on the color axis, assuming no rate suppression and a monochromatic mass function. We also include the fractional error on distance reached in the bottom subplot.

theoretical frequency track for a system with chirp mass \mathcal{M} and starting frequency $f_{\text{gw},x=0}$.

Even though each configuration was constructed to be sensitive to a particular \mathcal{M} and f_0 [45], we can actually probe a wide range of chirp masses and starting frequencies in each Hough map. Within a given Hough map j ($j \in [1, N_{\text{PM}}]$) for a particular configuration i ($i \in [1, N_{\text{config}}]$), all coincident candidates selected with a chirp mass \mathcal{M}_k and starting frequency f_l are assigned a critical ratio ($CR_{i,j,k,l}$). Using the Feldman-Cousins approach to set upper limits, which ensures perfect coverage at a given confidence level, $CR_{i,j,k,l}$ is mapped to an “inferred” positive-definite CR based on the upper value of Table 10 in [68] at 95% confidence. This approach produces consistent limits compared to those obtained by injecting simulated signals in real data [45,46,69,70]. Because $CR_{i,j,k,l}$ is found for LHO and LLO separately, we conservatively use the maximum of the two in Eq. (4) after applying the Feldman-Cousins approach.

Thus, we compute a distance reach $d_{i,j,k,l}$ for all 10^7 candidates returned from the first step of the search. We then select ~ 100 chirp masses \mathcal{M}_s that cover the searched parameter space at which we set upper limits, and, at each \mathcal{M}_s , in each configuration, take the median of the distance reaches over all frequencies and Hough maps (i.e., over T_{obs}): $d_{i,s} = \text{median}_{j,l}(d_{i,k=s,j,l})$. Essentially, our procedure corresponds to the median sensitivity of the search over time.

We then have one distance reach per configuration per \mathcal{M}_s . Some configurations will be more sensitive than others to certain chirp masses, though they search overlapping chirp-mass ranges; therefore, we take the maximum distance for each chirp mass as the upper limit, i.e., $d_s = \max_i(d_{i,s}) = d_{\text{max},95\%}(\mathcal{M}_s)$.

We then compute the spacetime volume $\langle VT \rangle$ of nearby PBH binaries and their rate density $\mathcal{R}_{95\%}$ [49,71,72]

$$\langle VT \rangle = \frac{4}{3} \pi d_{\text{max},95\%}^3 T_{\text{obs}}, \quad (5)$$

$$\mathcal{R}_{95\%} = \frac{3.0}{\langle VT \rangle}, \quad (6)$$

where $T_{\text{obs}} = 126$ days (adjusted for the detector duty cycle of 70%).

The upper limits on $d_{\text{max},95\%}$ and $\mathcal{R}_{95\%}$ are shown in Figs. 3 and 4 for the equal-mass and asymmetric mass-ratio cases, respectively. Note that these figures look different because we only place limits when we can ensure that the OPN waveform does not differ by more than one frequency bin from the 3.5 PN waveform during T_{PM} [45]. This makes asymmetric mass ratio systems harder to constrain than equal-mass ones, since the mass ratio enters at 1 PN [49].

Constraints on primordial black holes: To specialize our results to PBHs, we use the formulas from [73,74] for the cosmological merger rates that assume a purely Poissonian PBH spatial separation at formation, given by

$$\mathcal{R}_{\text{prim}}^{\text{cos}} \approx 1.6 \times 10^{-12} \text{ kpc}^{-3} \text{ yr}^{-1} f_{\text{sup}} f_{\text{PBH}}^{53/37} f(m_1) f(m_2) \times \left(\frac{m_1 + m_2}{M_{\odot}} \right)^{-32/37} \left[\frac{m_1 m_2}{(m_1 + m_2)^2} \right]^{-34/37}, \quad (7)$$

which correspond to the rate per unit of logarithmic mass of the two binary black hole components m_1 and m_2 . $f(m)$ is the mass distribution function of PBHs normalized to one, and f_{sup} accounts for rate suppression due to the gravitational influence of early forming PBH clusters, nearby

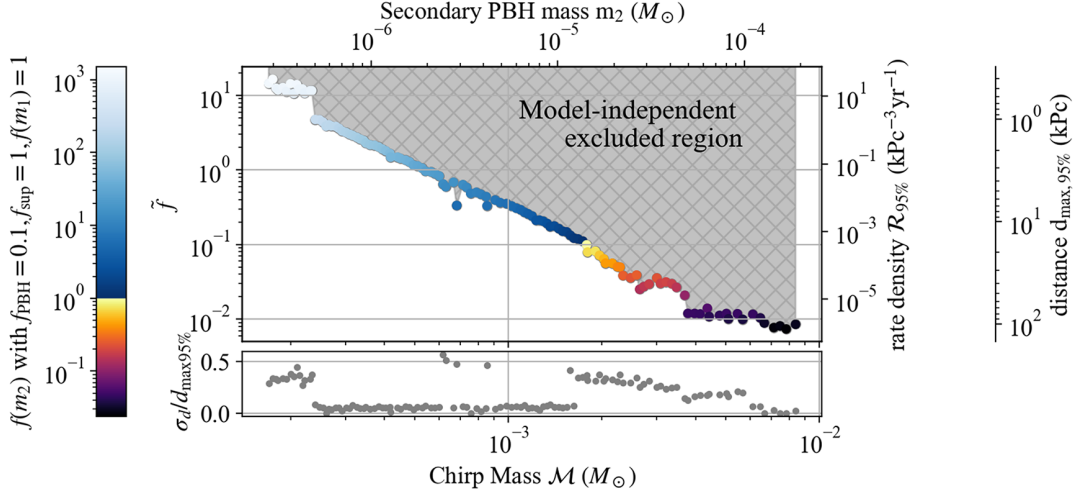


FIG. 4. Same as Fig. 3, but for asymmetric mass-ratio binaries. Model-dependent limits on $f(m_2)$ are shown on the color axis, assuming no rate suppression, $f(m_1) \sim 1$, and $f_{\text{PBH}} = 0.1$.

PBHs and matter inhomogeneities [73]. As in [47], we calculate the expected merging rates locally by assuming a constant local DM density of $\sim 10^{16} M_\odot \text{Mpc}^{-3}$ [75] consistent with the galactic DM profile. In this way, we obtain $\mathcal{R} = 3.3 \times 10^5 \mathcal{R}_{\text{prim}}^{\text{cos}}$ [69].

Values for f_{sup} vary depending on how wide the mass function is, how high the mass ratio and eccentricity of the binary are, and whether external tidal fields affect binary evolution [29,73,74,76,77]. We therefore provide limits on an effective parameter \tilde{f} , defined to be model agnostic:

$$\tilde{f}^{53/37} \equiv f_{\text{sup}} f(m_1) f(m_2) f_{\text{PBH}}^{53/37}. \quad (8)$$

First, we constrain equal-mass PBH merger rate densities and denote this mass m_{PBH} , for which

$$\mathcal{R} = 1.04 \times 10^{-6} \text{ kpc}^{-3} \text{ yr}^{-1} \left(\frac{m_{\text{PBH}}}{M_\odot} \right)^{-32/37} \tilde{f}_{\text{equal}}^{53/37}. \quad (9)$$

Upper limits on \tilde{f} are shown in Fig. 3, which are the first to probe $\tilde{f} < 1$. We also provide constraints on f_{PBH} assuming a monochromatic mass function and no rate suppression, which is below 1 for $m_{\text{PBH}} \gtrsim 2 \times 10^{-3} M_\odot$.

We can also place constraints on systems with highly asymmetric mass ratios, assuming negligible eccentricity, for which formation rates are larger by several orders of magnitude. Since PBHs are well motivated by observations of merging black holes in the stellar-mass range, we consider the merging rate densities of systems with $m_1 = 2.5 M_\odot$ [18,19,29], and $m_2 \ll m_1$:

$$\begin{aligned} \mathcal{R} &= 5.28 \times 10^{-7} \text{ kpc}^{-3} \text{ yr}^{-1} \left(\frac{m_1}{M_\odot} \right)^{-32/37} \\ &\times \left(\frac{m_2}{m_1} \right)^{-34/37} \tilde{f}_{\text{asymm}}^{53/37}, \end{aligned} \quad (10)$$

and constrain \tilde{f}_{asymm} as a function of m_2 in Fig. 4.

To constrain $f(m_2)$, we assume that the mass function is dominated by m_1 , i.e., $f(m_1) \approx 1$, which would be expected for broad mass functions affected by the QCD transition, implying $\tilde{f} = f_{\text{PBH}} [f(m_2)]^{37/53} f_{\text{sup}}^{37/53}$. If we assume a model in which $f_{\text{PBH}} = 0.1$ and $f_{\text{sup}} = 1$, we can translate these limits to constrain $f(m_2)$, which are also shown in Fig. 4. We see exclusions ($f(m_2) < 1$) when $m_2 \gtrsim 10^{-5} M_\odot$.

Conclusions—We presented results from the first-ever search for GWs from inspiraling planetary-mass PBH binaries. Depending on the chirp mass, we could detect binary PBHs that formed between [0.1,100] kpc away. Furthermore, we show that $f_{\text{PBH}} < 0.1$ for equal-mass PBH binaries with $m_{\text{PBH}} \sim [5 \times 10^{-3}, 2 \times 10^{-2}] M_\odot$, assuming no rate suppression and monochromatic mass functions. For asymmetric mass ratio systems, we constrain $f(m_2) < 0.1$ if $m_1 = 2.5 M_\odot$ and $m_2 \gtrsim 1.5 \times 10^{-5} M_\odot$, assuming $f_{\text{PBH}} = 0.1$. These limits are conservative with respect to those obtained with injections [45]. Furthermore, a major benefit of our formulation of upper limits is that they can be applied to *any* exotic compact object formation models, e.g., strange quark star inspirals [78], or a PBH inspiral inside a compact object [79].

However, our results neglect eccentricity of the binary, which could induce changes in the waveform, meaning that we would need to modify our method, or instead employ a model-agnostic one [49]. Furthermore, our limits on f_{PBH} and $f(m_2)$ should be reevaluated if non-Poissonian clustering, e.g., from primordial non-Gaussianity in the initial curvature distribution, occurs. Our work motivates future searches of planetary- and asteroid-mass PBH binaries, and our results will continue to improve when new data become available.

Acknowledgments—This material is based upon work supported by NSF’s LIGO Laboratory, which is a major

facility fully funded by the National Science Foundation. We would like to thank the Rome Virgo group for the tools necessary to perform these studies, such as the development of the original frequency-Hough transform and the development of the short FFT databases. Additionally we would like to thank Luca Rei for managing data transfers. This research has made use of data, software, and/or web tools obtained from the Gravitational Wave Open Science Center, a service of LIGO Laboratory, the LIGO Scientific Collaboration, and the Virgo Collaboration. LIGO Laboratory and Advanced LIGO are funded by the U.S. National Science Foundation (NSF) as well as the Science and Technology Facilities Council (STFC) of the United Kingdom, the Max-Planck-Society (MPS), and the State of Niedersachsen/Germany for support of the construction of Advanced LIGO and construction and operation of the GEO600 detector. Additional support for Advanced LIGO was provided by the Australian Research Council. Virgo is funded, through the European Gravitational Observatory (EGO), by the French Centre National de Recherche Scientifique (CNRS), the Italian Istituto Nazionale della Fisica Nucleare (INFN) and the Dutch Nikhef, with contributions by institutions from Belgium, Germany, Greece, Hungary, Ireland, Japan, Monaco, Poland, Portugal, and Spain. We also wish to acknowledge the support of the INFN-CNAF computing center for its help with the storage and transfer of the data used in this Letter. F. D. L. is supported by a FRIA (Fonds pour la formation à la Recherche dans l'Industrie et dans l'Agriculture) Grant of the Belgian Fund for Research, F. R. S.-FNRS (Fonds de la Recherche Scientifique-FNRS). This work is partially supported by ICSC-Centro Nazionale di Ricerca in High Performance Computing, Big Data and Quantum Computing, funded by European Union-NextGenerationEU.

Data availability—A data release for this work is available in a Zenodo repository [80].

-
- [1] J. Aasi, B. Abbott, R. Abbott, T. Abbott, M. Abernathy, K. Ackley, C. Adams, T. Adams, P. Addesso, R. Adhikari *et al.*, *Classical Quantum Gravity* **32**, 074001 (2015).
- [2] F. Acernese, M. Agathos, K. Agatsuma, D. Aisa, N. Allemandou, A. Allocca, J. Amarni, P. Astone, G. Balestri, G. Ballardin *et al.*, *Classical Quantum Gravity* **32**, 024001 (2014).
- [3] B. Abbott *et al.* (LIGO Scientific and Virgo Collaborations), *Phys. Rev. Lett.* **116**, 061102 (2016).
- [4] B. Abbott *et al.* (LIGO Scientific and Virgo Collaborations), *Phys. Rev. X* **6**, 041015 (2016); **8**, 039903(E) (2018).
- [5] B. P. Abbott *et al.* (LIGO Scientific and Virgo Collaborations), *Phys. Rev. Lett.* **116**, 241103 (2016).
- [6] B. P. Abbott *et al.* (LIGO Scientific and Virgo Collaborations), *Phys. Rev. Lett.* **118**, 221101 (2017); **121**, 129901(E) (2018).
- [7] B. P. Abbott *et al.* (LVC Collaboration), *Phys. Rev. Lett.* **119**, 141101 (2017).
- [8] B. P. Abbott *et al.* (LIGO Scientific and Virgo Collaborations), *Astrophys. J.* **851**, L35 (2017).
- [9] B. P. Abbott *et al.* (LIGO Scientific and Virgo Collaborations), *Phys. Rev. X* **9**, 031040 (2019).
- [10] R. Abbott *et al.* (LIGO Scientific and Virgo Collaborations), *Phys. Rev. D* **102**, 043015 (2020).
- [11] B. Abbott *et al.* (LIGO Scientific and Virgo Collaborations), *Astrophys. J. Lett.* **892**, L3 (2020).
- [12] R. Abbott *et al.* (LIGO Scientific and Virgo Collaborations), *Astrophys. J.* **896**, L44 (2020).
- [13] R. Abbott *et al.* (LIGO Scientific and Virgo Collaborations), *Phys. Rev. Lett.* **125**, 101102 (2020).
- [14] R. Abbott *et al.* (LIGO Scientific and Virgo Collaborations), *Astrophys. J.* **900**, L13 (2020).
- [15] S. Bird, I. Cholis, J. B. Muñoz, Y. Ali-Haïmoud, M. Kamionkowski, E. D. Kovetz, A. Raccanelli, and A. G. Riess, *Phys. Rev. Lett.* **116**, 201301 (2016).
- [16] S. Clesse and J. García-Bellido, *Phys. Dark Universe* **15**, 142 (2017).
- [17] M. Sasaki, T. Suyama, T. Tanaka, and S. Yokoyama, *Phys. Rev. Lett.* **117**, 061101 (2016); **121**, 059901(E) (2018).
- [18] B. Carr, S. Clesse, J. García-Bellido, and F. Kühnel, *Phys. Dark Universe* **31**, 100755 (2021).
- [19] C. T. Byrnes, M. Hindmarsh, S. Young, and M. R. S. Hawkins, *J. Cosmol. Astropart. Phys.* **08** (2018) 041.
- [20] K. Jedamzik, *J. Cosmol. Astropart. Phys.* **09** (2020) 022.
- [21] K. Jedamzik, *Phys. Rev. Lett.* **126**, 051302 (2021).
- [22] V. De Luca, G. Franciolini, and A. Riotto, *Phys. Rev. Lett.* **126**, 041303 (2021).
- [23] A. Escrivà, F. Kühnel, and Y. Tada, *Black Holes in the Era of Gravitational-Wave Astronomy* (Elsevier, New York, 2024).
- [24] Y. Ali-Haïmoud, E. D. Kovetz, and M. Kamionkowski, *Phys. Rev. D* **96**, 123523 (2017).
- [25] A. Hall, A. D. Gow, and C. T. Byrnes, *Phys. Rev. D* **102**, 123524 (2020).
- [26] V. De Luca, V. Desjacques, G. Franciolini, and A. Riotto, *J. Cosmol. Astropart. Phys.* **11** (2020) 028.
- [27] S. Clesse and J. García-Bellido, *Phys. Dark Universe* **22**, 137 (2018).
- [28] C. Boehm, A. Kobakhidze, C. A. J. O'hare, Z. S. C. Picker, and M. Sakellariadou, *J. Cosmol. Astropart. Phys.* **03** (2021) 078.
- [29] S. Clesse and J. Garcia-Bellido, *Phys. Dark Universe* **38**, 101111 (2022).
- [30] E. Bagui *et al.* (LISA Cosmology Working Group Collaboration), [arXiv:2310.19857](https://arxiv.org/abs/2310.19857).
- [31] T. S. Yamamoto, R. Inui, Y. Tada, and S. Yokoyama, *Phys. Rev. D* **109**, 103514 (2024).
- [32] J. C. Niemeyer and K. Jedamzik, *Phys. Rev. Lett.* **80**, 5481 (1998).
- [33] K. Jedamzik, *Phys. Rev. D* **55**, R5871 (1997).
- [34] B. P. Abbott *et al.* (LIGO Scientific and Virgo Collaborations), *Phys. Rev. Lett.* **121**, 231103 (2018).
- [35] B. Abbott, R. Abbott, T. Abbott, S. Abraham, F. Acernese, K. Ackley, C. Adams, R. Adhikari, V. Adya, C. Affeldt *et al.*, *Phys. Rev. Lett.* **123**, 161102 (2019).

- [36] A. H. Nitz and Y.-F. Wang, *Phys. Rev. Lett.* **126**, 021103 (2021).
- [37] C. Horowitz, M. Papa, and S. Reddy, *Phys. Lett. B* **800**, 135072 (2020).
- [38] A. H. Nitz and Y.-F. Wang, *Phys. Rev. Lett.* **127**, 151101 (2021).
- [39] R. Abbott *et al.* (LIGO Scientific, Virgo, and KAGRA Collaborations), *Phys. Rev. Lett.* **129**, 061104 (2022).
- [40] R. Abbott *et al.* (LIGO Scientific, Virgo, and KAGRA Collaborations), *Mon. Not. R. Astron. Soc.* **524**, 5984 (2023); **526**, 6234(E) (2023).
- [41] M. Ebersold and S. Tiwari, *Phys. Rev. D* **101**, 104041 (2020).
- [42] K. S. Phukon, G. Baltus, S. Caudill, S. Clesse, A. Depasse, M. Fays, H. Fong, S. J. Kapadia, R. Magee, and A. J. Tanasijczuk, [arXiv:2105.11449](https://arxiv.org/abs/2105.11449).
- [43] M. Prunier, G. Morrás, J. F. N. n. Siles, S. Clesse, J. García-Bellido, and E. Ruiz Morales, [arXiv:2311.16085](https://arxiv.org/abs/2311.16085).
- [44] A. H. Nitz and Y.-F. Wang, *Astrophys. J.* **915**, 54 (2021).
- [45] A. L. Miller, N. Aggarwal, S. Clesse, F. De Lillo, S. Sachdev, P. Astone, C. Palomba, O. J. Piccinni, and L. Pierini (to be published).
- [46] A. Miller *et al.*, *Phys. Rev. D* **98**, 102004 (2018).
- [47] A. L. Miller *et al.*, *Phys. Rev. D* **103**, 103002 (2021).
- [48] M. Andrés-Carcasona, O. J. Piccinni, M. Martínez, and L.-M. Mir, *Proc. Sci.*, EPS-HEP2023 (2023) 067.
- [49] G. Alestas, G. Morras, T. S. Yamamoto, J. Garcia-Bellido, S. Kuroyanagi, and S. Nesseris, *Phys. Rev. D* **109**, 123516 (2024).
- [50] D. Croon, D. McKeen, N. Raj, and Z. Wang, *Phys. Rev. D* **102**, 083021 (2020).
- [51] H. Niikura, M. Takada, S. Yokoyama, T. Sumi, and S. Masaki, *Phys. Rev. D* **99**, 083503 (2019).
- [52] P. Tisserand *et al.* (EROS-2 Collaboration), *Astron. Astrophys.* **469**, 387 (2007).
- [53] M. R. S. Hawkins, *Astron. Astrophys.* **633**, A107 (2020).
- [54] S. Bhatiani, X. Dai, and E. Guerras, *Astrophys. J.* **885**, 77 (2019).
- [55] J. García-Bellido and S. Clesse, *Phys. Dark Universe* **19**, 144 (2018).
- [56] J. Calcino, J. Garcia-Bellido, and T. M. Davis, *Mon. Not. R. Astron. Soc.* **479**, 2889 (2018).
- [57] K. M. Belotsky, V. I. Dokuchaev, Y. N. Eroshenko, E. A. Esipova, M. Y. Khlopov, L. A. Khromykh, A. A. Kirillov, V. V. Nikulin, S. G. Rubin, and I. V. Svadkovsky, *Eur. Phys. J. C* **79**, 246 (2019).
- [58] M. Trashorras, J. García-Bellido, and S. Nesseris, *Universe* **7**, 18 (2021).
- [59] M. Maggiore, *Gravitational Waves: Volume 1: Theory and Experiments* (Oxford University Press, New York, 2008), Vol. 1.
- [60] L. Sun *et al.*, *Classical Quantum Gravity* **37**, 225008 (2020).
- [61] F. Acernese *et al.* (Virgo Collaboration), *Classical Quantum Gravity* **35**, 205004 (2018).
- [62] G. Vajente, Y. Huang, M. Isi, J. C. Driggers, J. S. Kissel, M. J. Szczepanczyk, and S. Vitale, *Phys. Rev. D* **101**, 042003 (2020).
- [63] R. Abbott *et al.* (LIGO Scientific and Virgo Collaborations), *Phys. Rev. X* **11**, 021053 (2021).
- [64] D. Davis *et al.* (LIGO Collaboration), *Classical Quantum Gravity* **38**, 135014 (2021).
- [65] P. Astone, A. Colla, S. D’Antonio, S. Frasca, and C. Palomba, *Phys. Rev. D* **90**, 042002 (2014).
- [66] P. Astone, S. Frasca, and C. Palomba, *Classical Quantum Gravity* **22**, S1197 (2005).
- [67] O. J. Piccinni, P. Astone, S. D’Antonio, S. Frasca, G. Intini, P. Leaci, S. Mastrogiovanni, A. Miller, C. Palomba, and A. Singhal, *Classical Quantum Gravity* **36**, 015008 (2019).
- [68] G. J. Feldman and R. D. Cousins, *Phys. Rev. D* **57**, 3873 (1998).
- [69] A. L. Miller, S. Clesse, F. De Lillo, G. Bruno, A. Depasse, and A. Tanasijczuk, *Phys. Dark Universe* **32**, 100836 (2021).
- [70] R. Abbott *et al.* (LIGO Scientific, Virgo, and KAGRA Collaborations), *Phys. Rev. D* **106**, 102008 (2022).
- [71] A. L. Miller, N. Aggarwal, S. Clesse, and F. De Lillo, *Phys. Rev. D* **105**, 062008 (2022).
- [72] R. Biswas, P. R. Brady, J. D. E. Creighton, and S. Fairhurst, *Classical Quantum Gravity* **26**, 175009 (2009); **30**, 079502(E) (2013).
- [73] M. Raidal, C. Spethmann, V. Vaskonen, and H. Veermäe, *J. Cosmol. Astropart. Phys.* **02** (2019) 018.
- [74] G. Hütsi, M. Raidal, V. Vaskonen, and H. Veermäe, *J. Cosmol. Astropart. Phys.* **03** (2021) 068.
- [75] M. Weber and W. de Boer, *Astron. Astrophys.* **509**, A25 (2010).
- [76] Y. N. Eroshenko, *J. Phys. Conf. Ser.* **1051**, 012010 (2018).
- [77] I. Cholis, E. D. Kovetz, Y. Ali-Haïmoud, S. Bird, M. Kamionkowski, J. B. Muñoz, and A. Raccanelli, *Phys. Rev. D* **94**, 084013 (2016).
- [78] J. J. Geng, Y. F. Huang, and T. Lu, *Astrophys. J.* **804**, 21 (2015).
- [79] Z.-C. Zou and Y.-F. Huang, *Astrophys. J. Lett.* **928**, L13 (2022).
- [80] A. L. Miller *et al.*, Data release for gravitational wave constraints on planetary-mass primordial black holes using LIGO O3a data, Zenodo, [10.5281/zenodo.10724845](https://zenodo.org/record/10724845) (2024).